High-Throughput Screening Identifies Idasanutlin as a Resensitizing Drug for Venetoclax-Resistant Neuroblastoma Cells

Lindy Vernooij[1], Laurel T. Bate-Eya[1], Lindy K. Alles[1], Jasmine Y. Lee[2], Bianca Koopmans[1], Hunter C. Jonus[2], Nil A. Schubert[1], Linda Schild[1], Daphne Lelieveld[3], David A. Egan[3], Mark Kerstjens[4], Ronald W. Stam[1], Jan Koster[5], Kelly C. Goldsmith[2], Jan J. Molenaar[1], and M. Emmy M. Dolman[1,6]

ABSTRACT

Neuroblastoma tumors frequently overexpress the anti-apoptotic protein B-cell lymphoma/leukemia 2 (BCL-2). We previously showed that treating BCL-2–dependent neuroblastoma cells with the BCL-2 inhibitor venetoclax results in apoptosis, but unfortunately partial therapy resistance is observed. The current study describes the identification of drugs capable of resensitizing venetoclax-resistant neuroblastoma cells to venetoclax. To examine these effects, venetoclax resistance was induced in BCL-2–dependent neuroblastoma cell lines KCNR and SJNB12 by continuous exposure to high venetoclax concentrations. Non-resistant and venetoclax-resistant neuroblastoma cell lines were exposed to a 209-compound library in the absence and presence of venetoclax to identify compounds that were more effective in the venetoclax-resistant cell lines under venetoclax pressure. Top hits were further validated in combination with venetoclax using BCL-2–dependent neuroblastoma model systems. Overall, high-throughput drug screening identified the MDM2 inhibitor idasanutlin as a promising resensitizing agent for venetoclax-resistant neuroblastoma cell lines. Idasanutlin treatment induced BAX-mediated apoptosis in venetoclax-resistant neuroblastoma cells in the presence of venetoclax, whereas it caused p21-mediated growth arrest in control cells. *In vivo* combination treatment showed tumor regression and superior efficacy over single-agent therapies in a BCL-2–dependent neuroblastoma cell line xenograft and a patient-derived xenograft. However, xenografts less dependent on BCL-2 were not sensitive to venetoclax–idasanutlin combination therapy. This study demonstrates that idasanutlin can overcome resistance to the BCL-2 inhibitor venetoclax in preclinical neuroblastoma model systems, which supports clinical development of a treatment strategy combining the two therapies.

Introduction

The intrinsic apoptotic response is tightly regulated through a balance between anti-apoptotic and pro-apoptotic B-cell lymphoma/leukemia 2 (BCL-2) family members (1). Anti-apoptotic members, such as BCL-2, MCL-1, BCL-X_L and BCL-W, prevent apoptosis by sequestering pro-apoptotic BH3-only proteins like BIM, PUMA, NOXA, BAD and BID (2, 3). Some BH3-only proteins (e.g., PUMA, NOXA and BAD) interact with anti-apoptotic BCL-2 proteins to prevent them from sequestering other BH3-only proteins (e.g., BIM and BID) that can bind directly to pro-apoptotic proteins BAX and BAK to induce caspase-mediated cell death via mitochondrial outer membrane permeabilization. Apoptosis can be prevented by overexpression of anti-apoptotic BCL-2 family members that then bind to and inhibit the pro-apoptotic proteins, contributing to cancer cell survival (4–13).

Neuroblastomas are pediatric solid tumors that frequently express enhanced levels of the anti-apoptotic gene *BCL-2* (14, 15). Despite extensive treatment regimens, patients with neuroblastoma still have poor survival rates (16). A promising strategy to improve neuroblastoma treatment is to implement targeted therapy. Previously, our group showed that the selective BCL-2 inhibitor venetoclax (17) can induce a potent apoptotic response in BCL-2–dependent neuroblastoma cells via displacement of the pro-apoptotic protein BIM from BCL-2. *In vivo* studies confirmed these results, but also revealed that venetoclax monotherapy leads to a resistance mechanism, preventing complete tumor regression (18).

Several mechanisms for resistance to BCL-2 inhibitors have been described previously. In lymphoma cells, long-term exposure to venetoclax resulted in clonal selection of cells with mutations in the BH3 domain of BCL-2, leading to decreased affinity for venetoclax (19). Alternatively, resistance to venetoclax can occur via upregulation of other anti-apoptotic BCL-2 family members (18, 20, 21). Congruent with these findings, it was previously defined that acquired resistance of neuroblastoma cells to venetoclax occurs through MCL-1 upregulation, enabling recapturing of BIM released from BCL-2 upon venetoclax binding to BCL-2 (18).

In the current study, we aimed at identifying compounds that are capable of resensitizing venetoclax-resistant neuroblastoma cells to venetoclax, to improve its cancer cell killing potential.

[1]Princess Máxima Center for Pediatric Oncology, Utrecht, the Netherlands. [2]Department of Pediatrics, Emory University, Aflac Cancer and Blood Disorders Center at the Children's Healthcare of Atlanta, Atlanta, Georgia. [3]Department of Cell Biology, University Medical Center Utrecht, Utrecht, the Netherlands. [4]Department of Pediatric Oncology/Hematology, Erasmus MC-Sophia Children's Hospital, Rotterdam, the Netherlands. [5]Department of Oncogenomics, Amsterdam UMC, location AMC, Amsterdam, the Netherlands. [6]Children's Cancer Institute, Lowy Cancer Research Center, UNSW Sydney, Sydney, NSW, Australia.

Note: Supplementary data for this article are available at Molecular Cancer Therapeutics Online (http://mct.aacrjournals.org/).

L. Vernooij and L.T. Bate-Eya contributed equally as co-author of this article.

Corresponding Author: M. Emmy M. Dolman, Princess Máxima Center for Pediatric Oncology, Heidelberglaan 25, 3584 CT, Utrecht, the Netherlands. Phone: +31-6-16143181; E-mail: memdolman@gmail.com

Mol Cancer Ther 2021;20:1161–72

doi: 10.1158/1535-7163.MCT-20-0666

Materials and Methods

Chemicals

The Sequoia anti-neoplastic library containing 157 approved drugs used in cancer treatment and the SCREEN-WELL epigenetics library containing 43 epigenetic compounds were purchased from Sequoia Research Products and Enzo Life Sciences, respectively. Other targeted inhibitors were purchased from Selleck Chemicals, whereas the regularly used cytostatics were purchased from Sigma-Aldrich. Both compound libraries were reformatted to a single 384-well plate. AT7519 (multi-CDK inhibitor), JQ1 (BET bromodomain inhibitor), ceritinib (ALK inhibitor), ribociclib (CDK4/6 inhibitor), idasanutlin (MDM2 inhibitor), trametinib (MEK inhibitor), and YM155 (survivin inhibitor) were added to the reformatted library plate because these compounds target known genomic aberrations in neuroblastoma and were in (pre)clinical development as single-agent therapies for neuroblastoma. Venetoclax and navitoclax (BCL-2 inhibitors) were taken along as controls to confirm that the resistant cell lines were resistant to BCL-2 inhibition during the drug screen. For *in vivo* studies, venetoclax obtained from AbbVie was formulated in 10% ethanol/30% polyethylene glycol (PEG) 400/60% phosal 50 propylene glycol (PG; v/v/v) in final concentrations of 10 mg/mL. Idasanutlin obtained from Roche was formulated in 2% Klucel LF/0.1% Tween 80/0.09% methyl paraben/0.01% propyl paraben (v/v/v/v) in final concentrations of 15 mg/mL.

Cell culture

Human neuroblastoma cell lines KCNR (RRID: CVCL_7134) and SJNB12 (RRID: CVCL_1442) were chosen as the main cell lines used in this study because both cell lines have shown to express high BCL-2 levels in the absence of *TP53* mutations and respond well to venetoclax monotherapy (15, 18). Full profiling of both cell lines is available upon request. KCNR and SJNB12 were cultured as previously described (22) and tested every six weeks for *Mycoplasma* contamination using the MycoAlert detection kit (LT07–318, Lonza) and MycoAlert assay control set (LT07–518, Lonza). Cell culture protocols are described in detail in the Supplementary Materials and Methods.

Generation of venetoclax-resistant neuroblastoma cell lines

Venetoclax-resistant neuroblastoma cell lines were developed through long-term continuous exposure at the IC_{85} concentration (7.5 μmol/L for KCNR, 2.75 μmol/L for SJNB12). Following twice weekly routine maintenance splits or medium replenishment, cells were allowed to recover in venetoclax-free medium for 24 hours before adding fresh venetoclax. After three months, KCNR and SJNB12 cell lines cultured under venetoclax pressure replicated similarly to non-exposed control cells. Resistance was confirmed through dose–response curves and cell-cycle analysis (see below).

BCL-2 DNA sequence analysis

Genomic DNA from non-resistant KCNR and SJNB12 cells and venetoclax-resistant KCNR and SJNB12 cells under venetoclax pressure (IC_{85}) was extracted using chloroform and isopropanol. Isolated DNA was purified using a QIAamp DNA mini kit (Qiagen) and PCR-amplified with Taq polymerase (Invitrogen). Gene sequence analysis was then performed using the ABI PRISM 3730 sequencer (Applied Biosystems). Primers used for the gene sequence analysis are: Exon 1: F: GTCCAAGAATGCAAAGCACA, R: GAACGCTTTGTGGAGAGGAG. Exon 2: F: GCAGGATGCCTCTTTCTCTG, R: AGCCTGCAGCTTTGTTTCAT.

mRNA expression profiling

RNA was extracted from KCNR and SJNB12 non-resistant cells and venetoclax-resistant cells in the absence or presence of venetoclax using TRIzol (Invitrogen) following the manufacturer's protocols. Concentration and quality were determined using the RNA 6000 Nano assay on the Agilent 2100 Bioanalyzer (Agilent Technologies). Fragmentation of cRNA, hybridization to Human Genome U133 plus 2.0, microarrays and scanning were carried out according to the manufacturer's protocol (Affymetrix Inc.). The mRNA gene expression data were normalized with the MAS5.0 algorithm of the GCOS program (Affymetrix Inc.) and target intensity was set to 100. All data were analyzed using the R2 genomic analysis and visualization platform (http://r2.amc.nl).

High-throughput drug screening

Non-resistant and venetoclax-resistant cell lines were seeded in 384-well plates (8,000 cells/well for KCNR lines, 10,000 cells/well for SJNB12). Resistant cell lines were plated both in the presence or absence of venetoclax (IC_{85}). Cells were allowed to attach overnight before exposure to three different concentrations (10 nmol/L, 100 nmol/L, and 1 μmol/L) of library compounds using the Sciclone ALH 3000 liquid handling robot (Perkin Elmer). As vehicle control, cells were treated with equal volumes of DMSO. Cell viability was determined before and following 72 hours treatment using the MTT colorimetric assay (M2128, Sigma-Aldrich). Viability of vehicle control cells was set to 100%. For each compound in the library, the area under the dose–response curve (AUC) values and the sum of the percentage viable cells (sum %) observed after treatment with 10 nmol/L, 100 nmol/L, and 1 μmol/L were calculated for the non-resistant cells, venetoclax-resistant cells, and venetoclax-resistant cells under venetoclax pressure. Compounds for which the sum % was lower for the venetoclax-resistant cells under venetoclax pressure than for the non-resistant cells were considered resensitizing compounds.

Validation of the resensitizing effects of compounds

Non-resistant and venetoclax-resistant KCNR and SJNB12 neuroblastoma cell lines were seeded in quadruplicate as described above. After overnight incubation, KCNR and SJNB12 non-resistant cells and venetoclax-resistant cells in the absence and presence of venetoclax were treated with either eight concentrations of each compound or vehicle control (DMSO) using the Combi-Bulk Tecan HP D300 digital dispenser (Hewlett–Packard).

FACS analysis

To confirm the generation of venetoclax-resistant KCNR and SJNB12 cells, non-resistant and resistant cells were treated with vehicle control (DMSO) or venetoclax using a concentration gradient from 7.5 nmol/L to 10 μmol/L. To study the effects of idasanutlin on sub-G_1 induction in SJNB12, non-resistant cells, venetoclax-resistant cells, and venetoclax-resistant cells in the presence of venetoclax (IC_{85}) were treated with DMSO or 15.5 nmol/L to 1 μmol/L idasanutlin. For both FACS experiments, cells were seeded in 6-cm plates and incubated overnight. Subsequently, cells were treated for 72 hours and harvested for FACS analysis to determine the apoptotic sub-G_1 fraction. See Supplementary Materials and Methods for a detailed protocol.

In vitro western blotting

The following antibodies were ordered from Cell Signaling Technology (CST) and were used in a 1:1,000 dilution: BCL-2 (D55G8,

rabbit, #4223), MCL-1 (rabbit, #4572), BCL-X_L (54H6, rabbit, #2764), BCL-W (31H4, rabbit, #2724), BIM (C34C5, rabbit, #2933), PARP (rabbit, #9542), BAX (rabbit, #2774), BAK (rabbit, #3814) and PUMA (rabbit, #4976). The α-tubulin antibody (DM1A, mouse, #3873) was diluted 1:10,000. Other antibodies used in a 1:1,000 dilution: p21 (rabbit, ab109520, Abcam), p53 (D0–7, mouse, Neomarkers), NOXA (rabbit, ab140129, Abcam), BID (rabbit, ab32060, Abcam), and MDM2 (N-20, rabbit, SC-813, Santa Cruz Biotechnology). Secondary antibodies used in a 1:10,000 dilution: Horseradish peroxidase (HRP)–conjugated goat anti-rabbit (NA9340V) and goat anti-mouse (NXA931) antibodies (GE Healthcare). See Supplementary Materials and Methods for a detailed protocol.

In vitro co-immunoprecipitation and immunoblotting

Non-resistant KCNR and SJNB12 cells and venetoclax-resistant cells in the absence and presence of venetoclax were seeded in T175 flasks. For the detection of BIM/BCL-2 and BIM/MCL-1 complexes, cells were harvested using TrypLE express enzyme (12605036, Thermo Fisher Scientific) followed by washing with PBS. For all samples, total cell lysates were prepared in 2% CHAPS buffer [1 mol/L HEPES, 150 mmol/L NaCl, 5 mmol/L EDTA, 5% (w/v) sodium glycerol phosphate and 2% (w/v) CHAPS]. Samples were allowed to lyse overnight at 4°C, followed by centrifugation for 20 minutes at 15,000 rpm, 4°C to pellet debris. Supernatants were precleared using protein A-agarose beads (before BCL-2 co-immunoprecipitation) or protein G-agarose beads (before MCL-1 co-immunoprecipitation). Equal protein amounts (i.e., 1 mg) were then incubated for 1.5 hours with either a BCL-2 antibody, an MCL-1 antibody or a FlagTag antibody followed by adding the solution to protein A- or G-agarose beads (Roche) for 24 hours at 4°C to immunoprecipitate the desired protein complexes. The following antibodies were used in a 1:140 dilution for immunoprecipitation: BCL-2 (D55G8, rabbit, #4223, CST), MCL-1 (RC13, mouse, #MABC43, Merck Millipore), DYKDDDDK Tag (rabbit, #2368, CST) or DYKDDDDK Tag (mouse, 9A3, #8146, CST). Co-immunoprecipitated proteins were isolated by repeatedly spinning down (2 minutes, 8,000 rpm, 4°C) and washing of the sample–antibody–bead complexes. Samples were analyzed by western blot analysis as described above.

In vivo efficacy in classical cell line xenograft and patient-derived xenograft models

Experiments involving cell line–derived xenografts were performed with permission from and according to the standards of the Dutch animal ethics committee (DAG102776, DAG103059, DAG309AA and DAG309AB). As *in vivo* engraftment of SJNB12 did not lead to tumor formation, BCL-2–dependent neuroblastoma cell lines KCNR and KP–N–YN were selected for the generation of xenograft mouse models. Single-cell suspensions containing 5×10^6 cells were resuspended in Matrigel/PBS (1:1 ratio) and subcutaneously injected into both flanks of female NMRI nu^-/nu^- mice (6–15-weeks-old, 20–30 g) obtained from Charles River Laboratories. Tumor volume was recorded twice weekly by caliper measurements ($\text{tumor}_{\text{small side}} \times \text{tumor}_{\text{small side}} \times \text{tumor}_{\text{large side}} \times \pi/6$). When the tumors reached approximately 1,000 mm^3, tumors were excised, chunked, and serially xenotransplanted in recipient mice. Experimental treatment started when transplanted tumors of recipient mice reached approximately 250 mm^3. Mice were randomly divided into four groups: (i) vehicle venetoclax + vehicle idasanutlin, (ii) 100 mg/kg/day venetoclax + vehicle idasanutlin, (iii) 25 mg/kg/day idasanutlin + vehicle venetoclax, (iv) venetoclax combined with idasanutlin. For KCNR, a fifth group (i.e., delayed combination group) was included, receiving one-week venetoclax monotherapy followed by two weeks combination treatment. Mice ($n = 7$ per group for KCNR and $n = 6$ per group for KP–N–YN) were treated daily for up to three weeks to follow treatment effects on tumor growth and regression.

For the patient-derived xenograft (PDX) models, experiments were performed with permission from the Emory institutional animal care and use committee. Viably frozen tumor pieces of CHOA-NBX-4 and COG-N-424x PDXs were disaggregated to generate a single-cell suspension. Cells (4×10^6) were subsequently resuspended in Matrigel at a 1:2 ratio and subcutaneously injected into the flank of female nu^-/nu^- athymic mice (5–6-weeks-old, ∼18 g) obtained from The Jackson Laboratory. Tumor volume was recorded three times weekly by caliper measurements ($L \times W \times H \times \pi/6$). When tumor volume reached approximately 250 mm^3, mice were assigned to one of four treatment arms, as described above for the classical *in vivo* models. Mice ($n = 4$–6 for CHOA-NBX-4, $n = 4$ for COG-N-424x) were treated daily for three weeks to follow treatment effects on tumor growth and regression.

Western blotting on xenograft tumor samples

The following antibodies were used: p21 (rabbit, #2947, CST), p53 (mouse, SC-126, Santa Cruz Biotechnology), MDM2 (rabbit, #86934, CST), BCL-X_L (rabbit, #2762, CST), BCL-2 (rabbit, SC-492, Santa Cruz Biotechnology), MCL-1 (rabbit, ADI-AAP-240-F, ENZO), BIM (rabbit, AB17003, Millipore), BAX (rabbit, #2772, CST), PARP (rabbit, #9542, CST), GAPDH (rabbit, #2118, CST), anti-rabbit-HRP (goat, HAF008, R&D Systems), and anti-mouse-HRP (goat, 554002, BD Biosciences). All antibodies were used in a 1:1,000 dilution. β-Actin (rabbit, #4970, CST) antibody was used as a loading control and diluted 1:10,000. See Supplementary Materials and Methods for detailed protocols. BAX detection in KCNR xenografts was carried out following the protocol for *in vitro* western blotting.

Co-immunoprecipitation on xenograft tumor samples

Immunoprecipitation was performed using 5 μg of the following antibodies: MCL-1 (mouse, 559027, BD Biosciences) and BCL-2 (mouse, M088729–2, Dako). The following antibodies were used for immunoblotting: BIM (rabbit, #2933, CST, 1:500), MCL-1 (rabbit, ADI-AAP-240-F, Enzo Life Sciences, 1:1,000), BCL-2 (rabbit, SC-492, Santa Cruz Biotechnology, 1:1,000), anti–rabbit-HRP (goat, HAF008, R&D Systems, 1:1,000) and anti–rabbit-HRP [goat, SC-45040 (discontinued), Santa Cruz Biotechnology, 1:5,000]. See Supplementary Materials and Methods for detailed protocols. Detection of BIM/BCL-2 complex levels in KCNR was carried out as described previously in the section *in vitro* co-immunoprecipitation, with minor modifications due to prior tumor homogenization.

Results

Long-term continuous exposure of BCL-2-dependent neuroblastoma cells to high venetoclax concentrations confirms MCL-1–mediated resistance

To investigate whether neuroblastoma cells with acquired resistance to venetoclax can be resensitized again to the compound, wild-type BCL-2–dependent neuroblastoma cell lines KCNR and SJNB12 were made venetoclax-resistant by continuous exposure to IC_{85} concentrations of venetoclax (7.5 μmol/L for KCNR and 2.75 μmol/L for SJNB12). Resistance to venetoclax was confirmed by quantifiable shifts in venetoclax dose–response curves (**Fig. 1A**). IC_{50} values were 22 and 12 times higher, whereas LC_{50} values were

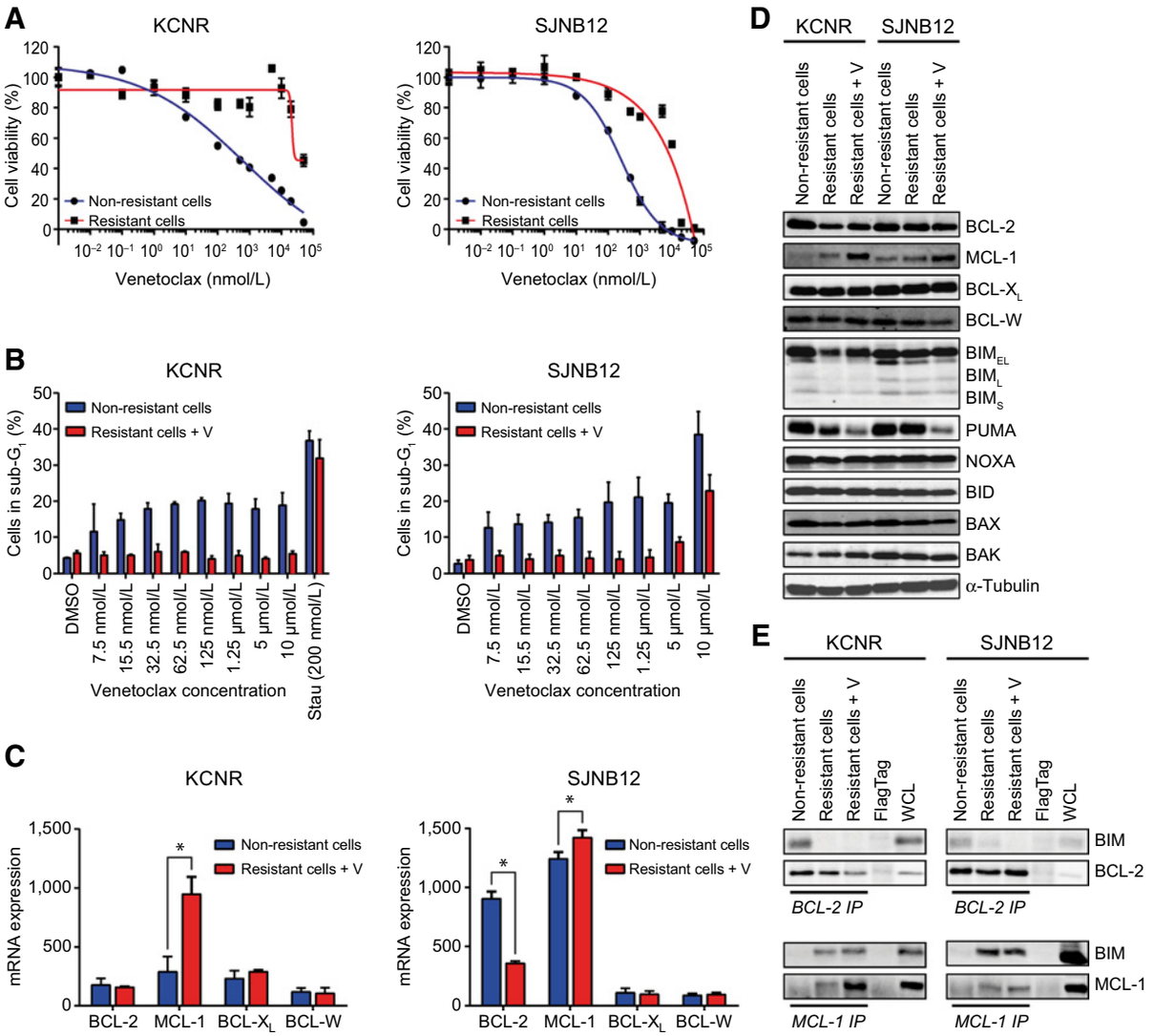

Figure 1.

Long-term continuous exposure of BCL-2–dependent neuroblastoma cell lines to high venetoclax concentrations results in MCL-1–mediated venetoclax resistance. **A,** Dose–response curves of venetoclax for non-resistant (blue) and venetoclax-resistant (red) KCNR and SJNB12 cells. Venetoclax effects on cell viability were established 72 hours after treatment using the MTT colorimetric assay. **B,** FACS analysis of the effects of venetoclax on sub-G_1 induction in non-resistant (blue) and venetoclax-resistant (red) KCNR and SJNB12 cells. Effects on sub-G_1 induction were measured after 72 hours treatment with increasing venetoclax concentrations. For KCNR, staurosporine was included as a positive control. Data represent the mean percentage of cells in sub-G_1 + SD of three replicate experiments. **C,** Affymetrix gene expression profiling of anti-apoptotic BCL-2 family members in non-resistant and resistant KCNR and SJNB12 cells in the presence of venetoclax. Data represent mean expression levels of triplicate samples + SD. Statistical differences between non-resistant and resistant cells in the presence of venetoclax were calculated using a one-tailed unpaired Student *t* test, with $P < 0.05$ as the minimal level of significance (indicated as *). **D,** Western blot analysis of anti-apoptotic and pro-apoptotic BCL-2 family members in non-resistant cell lines, venetoclax-resistant cell lines and venetoclax-resistant cell lines in the presence of venetoclax. α-Tubulin was used as a loading control. **E,** BIM/BCL-2 and BIM/MCL-1 complex levels in non-resistant cells, venetoclax-resistant cells and venetoclax-resistant cells in the presence of venetoclax. BIM/BCL-2 and BIM/MCL-1 complex levels were established by anti–BCL-2 and anti-MCL-1 immunoprecipitation, respectively, followed by western blotting for BIM. +V = venetoclax IC_{85} concentration (KCNR, 7.5 µmol/L and SJNB12, 2.75 µmol/L).

191 and 51 times higher for resistant versus non-resistant KCNR and SJNB12 cell lines, respectively (Supplementary Table S1). Furthermore, micromolar concentrations of venetoclax (i.e., ≥5 µmol/L) were required to induce an apoptotic response in venetoclax-resistant SJNB12 cells, whereas non-resistant control cells required nanomolar equivalents (i.e., 7.5 nmol/L) to induce a ≥2-fold increase in the sub-G_1 population (**Fig. 1B**). Venetoclax exposure at the highest concentration tested (10 µmol/L) was insufficient to induce sub-G_1 arrest in venetoclax-resistant KCNR cells (**Fig. 1B**).

Previously, we have shown that MCL-1 plays a pivotal role in venetoclax resistance. Therefore, validation experiments were performed to verify MCL-1–mediated resistance within this study (18). DNA sequence analysis of venetoclax-resistant cells did not identify mutations in the BH3 domain of BCL-2. Gene expression profiling of non-resistant and venetoclax-resistant KCNR and

SJNB12 cells under venetoclax pressure showed significantly increased *MCL-1* mRNA expression in the resistant cell lines (**Fig. 1C**). This coincided with elevated levels of MCL-1 protein in both models (**Fig. 1D**). Surprisingly, *BCL-2* gene and protein levels were not consistently downregulated. Lower *BCL-2* gene expression was observed for resistant SJNB12 cells (**Fig. 1C**; Supplementary Fig. S1), whereas reduced BCL-2 protein levels were seen for resistant KCNR cells (**Fig. 1D**). Similar analyses revealed no significant changes in gene and protein levels of the anti-apoptotic BCL-2 family members BCL-X_L and BCL-W (**Fig. 1C** and **D**). In addition, protein levels of pro-apoptotic BCL-2 family members largely remained unchanged between non-resistant and resistant cell lines, except for BIM and PUMA. Lower levels of BIM were observed in resistant KCNR cells and PUMA was down-regulated in both resistant cell lines under venetoclax pressure (**Fig. 1D**). BCL-2 immunoprecipitation followed by immunoblotting for BIM, confirmed displacement of BIM from BCL-2 in resistant KCNR and SJNB12 cells with and without venetoclax pressure (**Fig. 1E**). In line with our previously published observations upon short-term treatment of neuroblastoma cells with venetoclax (18), analysis of BIM/MCL-1 complex levels revealed that BIM released from BCL-2 was sequestrated by MCL-1 in the resistant cells (**Fig. 1E**). Together, these results support that MCL-1 plays an important role in the acquired resistance induced by long-term exposure of BCL-2-dependent neuroblastoma cells to venetoclax.

High-throughput screening identifies idasanutlin as a resensitizing agent for venetoclax-resistant neuroblastoma cells

To identify compounds that resensitize venetoclax-resistant neuroblastoma cells to venetoclax, we performed a high-throughput drug screen for non-resistant KCNR and SJNB12 cells, venetoclax-resistant KCNR and SJNB12 cells and venetoclax-resistant KCNR and SJNB12 cells in the presence of venetoclax. Cells were exposed for 72 hours to a compound library, containing three concentrations (10 nmol/L, 100 nmol/L and 1 μmol/L) of 157 approved drugs used in cancer treatment, 43 epigenetic regulators and 9 targeted compounds that are currently in (pre)clinical development for neuroblastoma treatment. Compounds that were more effective in the resistant cell lines under venetoclax pressure than in the non-resistant cell lines were considered resensitizing drugs (**Fig. 2A**).

Hit selection was performed by taking the top 40 resensitizing compounds and subsequently excluding all non-targeted compounds (except cytostatics regularly used in neuroblastoma treatment) and targeted compounds for which the percentage viable cells after treatment with the highest tested concentration (1 μmol/L) was still ≥20%. This yielded 11 and 13 hits for venetoclax-resistant KCNR and SJNB12, respectively (**Fig. 2B**).

Interestingly, both hit lists contained different inhibitors of the IGF-1R/PI3K/mTOR axis, including omipalisib (PI3K/mTOR inhibitor; KCNR and SJNB12), GSK-1904529A (IGF-1R inhibitor; KCNR), AZD-8055 (mTOR inhibitor; SJNB12), and NVP-BEZ235 (PI3K/mTOR inhibitor; SJNB12). In addition, two ALK inhibitors (i.e., ceritinib and NVP-TAE684) were identified as highly ranked resensitizing agents in the F1174 L ALK-mutated model system KCNR. As expected, these ALK inhibitors were not observed as hits in the ALK wild-type cell line SJNB12.

Besides omipalisib, idasanutlin (MDM2 inhibitor), flavopiridol (CDK inhibitor), and vorinostat (HDAC inhibitor) were the only overlapping targeted drugs between the two hit lists. For idasanutlin, omipalisib, and flavopiridol, the increase in efficacy between venetoclax-resistant and non-resistant cells was larger in the presence of venetoclax, confirming the occurrence of resensitization in addition to or instead of overcoming resistance. Overall, the best performing resensitizing compound idasanutlin (23) was selected for further validation *in vitro* and *in vivo*, as being the eighth and first hit for venetoclax-resistant KCNR and SJNB12 cells, respectively.

In vitro validation confirms the resensitizing potential of idasanutlin

The top resensitizing hit idasanutlin was tested more extensively *in vitro*, along with other resensitizing compounds, to validate the screening results using a low-throughput methodology. Targeted compounds for which synergy with BCL-2 inhibition has been previously described (20, 24–31) and regularly used cytostatics for neuroblastoma treatment (Supplementary Table S2) were also tested. For all compounds, IC_{50} values in non-resistant KCNR and SJNB12 cells and in venetoclax-resistant KCNR and SJNB12 cells in the absence and presence of venetoclax were determined from dose–response curves after 72 hours treatment (Supplementary Table S3). **Figure 3A** and **B** shows the top 15 resensitizing compounds for KCNR and SJNB12, determined by the largest fold decrease in IC_{50} value between resistant cells under venetoclax pressure and non-resistant cells. Results confirm the resensitizing potential of idasanutlin, with a 1.5-fold decrease in IC_{50} value for KCNR (i.e., 30 vs. 20 nmol/L) and an almost 20-fold decrease in IC_{50} value for SJNB12 (i.e., 1,011 vs. 52 nmol/L; **Fig. 3C**). For both neuroblastoma cell lines, only limited differences were observed in idasanutlin IC_{50} values between the venetoclax-resistant cells in the absence of venetoclax and the non-resistant cells. This supports the hypothesis that idasanutlin resensitizes venetoclax-resistant neuroblastoma cells to venetoclax, rather than overcoming venetoclax resistance. In line with the screening results, omipalisib and vorinostat were also found in the top 15 list of most potent resensitizing drugs for venetoclax-resistant KCNR and SJNB12 cells.

Idasanutlin induces growth arrest in non-resistant cells and apoptosis in venetoclax-resistant cells in the presence of venetoclax

Idasanutlin acts by inhibiting the interaction between MDM2 and the tumor-suppressor p53, thereby preventing p53 degradation (32, 33). For this reason, we first studied the effects of idasanutlin on p53 and MDM2 proteins levels. As expected, idasanutlin dose-dependently increased p53 and MDM2 in the non-resistant cells as well as the venetoclax-resistant cells in the absence and presence of venetoclax for both KCNR and SJNB12 (**Fig. 4A**). Because p53 is involved in both cell-cycle arrest and apoptosis, we also studied the effects of idasanutlin on p53 target genes p21 and BAX (34–36). Interestingly, in the non-resistant cells and venetoclax-resistant cells in the absence of venetoclax a stronger p21 upregulation was observed, whereas in the venetoclax-resistant cells in the presence of venetoclax a stronger BAX upregulation was observed upon idasanutlin treatment. These findings correspond with apoptosis induction in the venetoclax-resistant lines under venetoclax pressure demonstrated by the observed PARP cleavage (**Fig. 4A**) and higher sub-G_1 fraction after cell-cycle analysis (**Fig. 4B**; Supplementary Fig. S2). Taken together, *in vitro* results indicate that treating BCL-2–dependent neuroblastoma cells with a combination of venetoclax and idasanutlin is more effective in inducing an apoptotic response than either of the compounds alone.

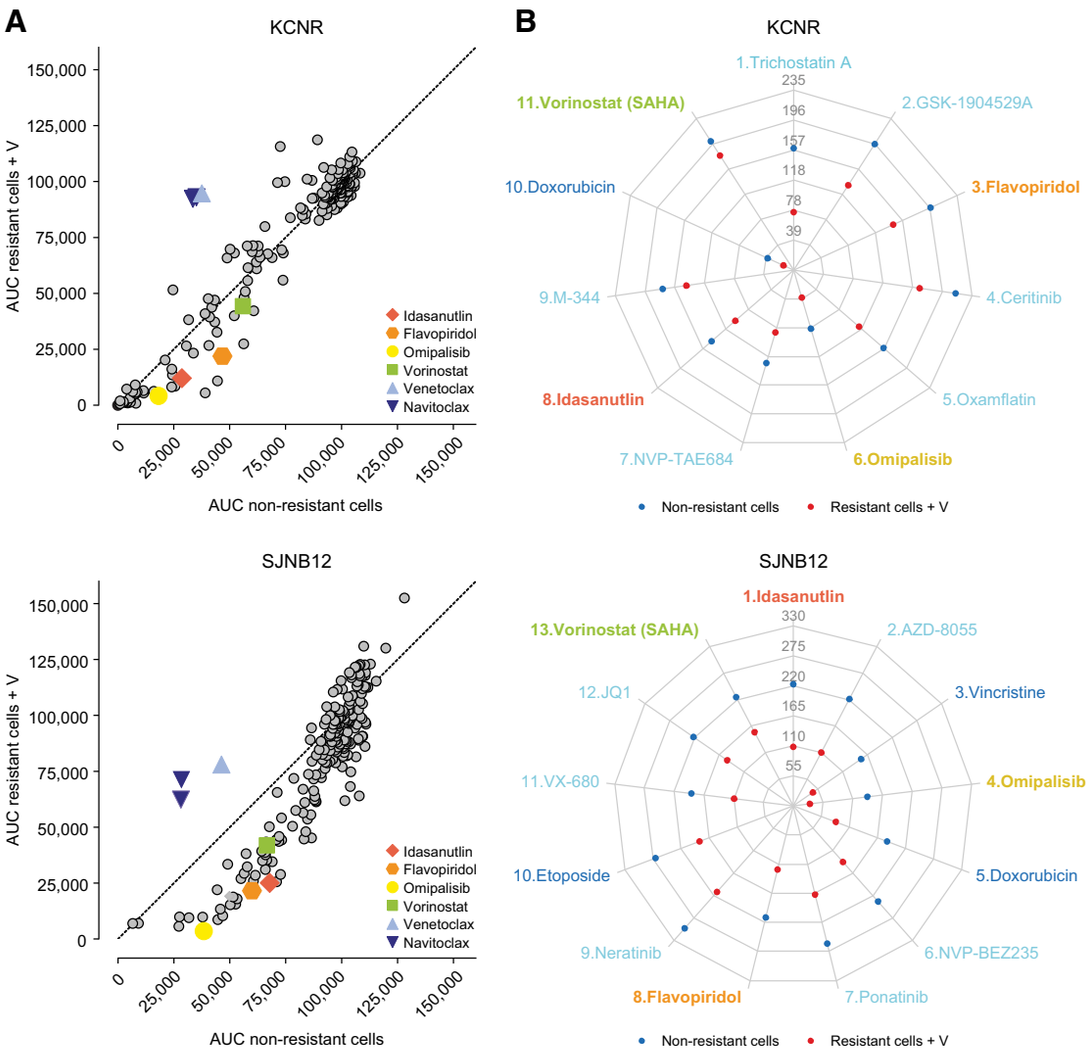

Figure 2.

High-throughput screening identifies drugs resensitizing neuroblastoma cells to venetoclax treatment. For each compound, the area under the dose–response curve (AUC) values and the sum of the percentage (sum %) viable cells observed after treatment with 10 nmol/L, 100 nmol/L, and 1 μmol/L were calculated for the non-resistant cells and venetoclax-resistant cells in the presence of venetoclax. **A,** Drug AUC values for non-resistant cells (*x*-axis) versus venetoclax-resistant cells in the presence of venetoclax (*y*-axis). Each dot represents a single compound. Compounds below the diagonal lines are more effective in the resistant cells under venetoclax pressure and are therefore considered potential resensitizing compounds. BCL-2 inhibitors venetoclax and navitoclax were taken along as controls. **B,** Radar charts showing the top hits for venetoclax resensitization in KCNR and SJNB12. Radar charts show the sum % viable cells for the non-resistant cells (blue dots) versus the venetoclax-resistant cells in the presence of venetoclax (red dots). Resensitizing hits are numbered from most potent to least potent. Drug name colors indicate overlapping hits between KCNR and SJNB12 (red, orange, yellow, and green), unique hits for KCNR or SJNB12 (light blue) or regularly used cytostatics in neuroblastoma treatment (dark blue). +V = venetoclax IC_{85} concentration (KCNR, 7.5 μmol/L and SJNB12, 2.75 μmol/L).

Venetoclax and idasanutlin combination therapy causes tumor regression in a BCL-2–dependent neuroblastoma xenograft model

The additional value of combining idasanutlin with venetoclax therapy was subsequently validated *in vivo* using BCL-2–dependent p53 wild-type KCNR xenografts. Mice were treated for three weeks with daily oral doses of 100 mg/kg venetoclax and/or 25 mg/kg idasanutlin. Both single-agent therapies and combination therapy with venetoclax and idasanutlin significantly inhibited tumor growth, with average changes in tumor volume of +78% (venetoclax), +186% (idasanutlin), and −80% (venetoclax + idasanutlin) versus +512% for the vehicle control (**Fig. 5A**; Supplementary Fig. S3B). Combination therapy demonstrated superior efficacy over either of the drugs alone, with 1/6 complete remission (CR), 2/6 very good partial responses (VGPR), and 3/6 partial regressions (PR) versus no response (NR in 1/6 and 3/7 mice, respectively) or progressive disease (PD in 5/6 and 4/7 mice, respectively) for venetoclax and idasanutlin monotherapy. Mice receiving one-week venetoclax monotherapy followed by two weeks combination therapy showed slightly less favorable responses compared with immediate addition of both compounds, with one VGPR, three PRs and three NRs. However, comparing immediate combination therapy with delayed combination did

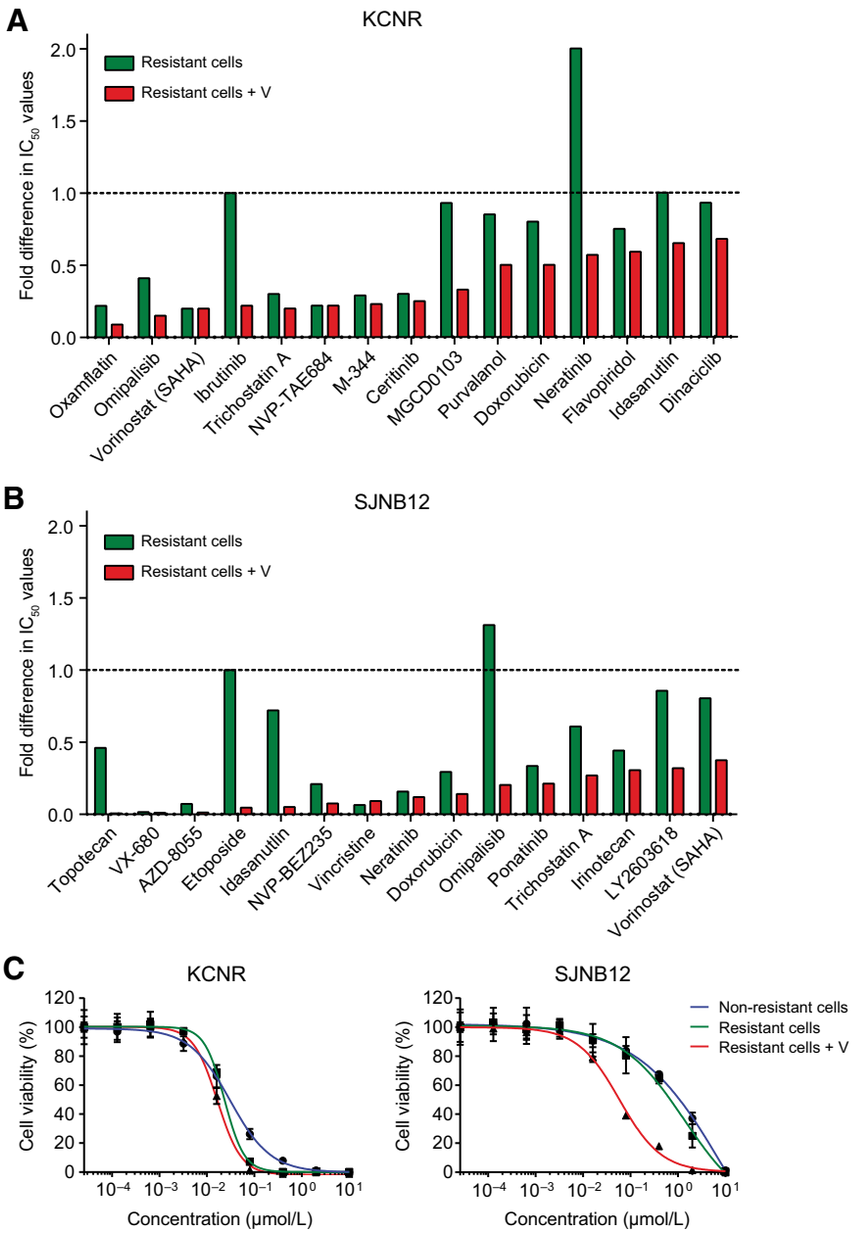

Figure 3.

In vitro validation studies confirm resensitization of venetoclax-resistant neuroblastoma cells to venetoclax by idasanutlin treatment. For combined hits from the high-throughput drug screen as well as targeted compounds for which synergy with BCL-2 inhibition has been described in literature and the regularly used cytostatics in neuroblastoma treatment, dose–response curves were established in non-resistant KCNR and SJNB12 cells and venetoclax-resistant KCNR and SJNB12 cells in the absence and presence of venetoclax to establish IC_{50} values. **A** and **B,** Fold difference in IC_{50} values between non-resistant cells and either venetoclax-resistant cells (green bars) or venetoclax-resistant cells under venetoclax pressure (red bars). Results are shown for the top 15 compounds showing the largest fold decrease in IC_{50} value between the non-resistant cells and the resistant cells in the presence of venetoclax for KCNR (**A**) and SJNB12 (**B**), respectively. **C,** Dose–response curves of the MDM2 inhibitor idasanutlin in non-resistant KCNR and SJNB12 cells (blue) and venetoclax-resistant KCNR and SJNB12 cells in the absence (green) or presence (red) of venetoclax. +V = venetoclax IC_{85} concentration (KCNR, 7.5 μmol/L and SJNB12, 2.75 μmol/L).

not lead to significant changes in the average tumor volume. Co-immunoprecipitation studies on tumor material harvested 4 hours after administration of the last doses, showed complete BIM release from BCL-2 in mice that received venetoclax alone or the immediate combination with idasanutlin (**Fig. 5B**). Interestingly, residual BIM/BCL-2 complex levels were observed in mice that received delayed combination therapy, which might explain the slightly less favorable response observed in this group (**Fig. 5B**). Additional western blot analysis revealed increased BAX levels in idasanutlin-treated tumors and an even more pronounced BAX upregulation in both combination arms (Supplementary Fig. S3D). Together, these results indicate that the observed tumor regression upon combination therapy might be the result of a dual effect on the intrinsic apoptotic pathway: BIM release from BCL-2 caused by venetoclax and p53-mediated activation of the pro-apoptotic BCL-2 family member BAX caused by idasanutlin.

Effects of venetoclax–idasanutlin combination therapy were also tested in mice with high BCL-2–expressing p53 wild-type KP–N–YN cell line–derived xenografts. Although average changes in tumor volume after three weeks treatment with venetoclax, idasanutlin or combination therapy (i.e., +119%, +138%, and +97%, respectively) were lower compared with the vehicle control (+236%), differences were not statistically significant (**Fig. 5A**; Supplementary Fig. S3B). Co-immunoprecipitation studies showed less pronounced BIM release from BCL-2 after venetoclax monotherapy or combination treatment compared with KCNR xenografts (**Fig. 5B**). Additional analysis of BIM/MCL-1 complex levels furthermore showed that BIM was already bound to MCL-1 in untreated xenografts and complex levels even raised upon combination treatment (Supplementary Fig. S3E). This indicates that KP–N–YN neuroblastoma xenografts are not solely BCL-2–dependent.

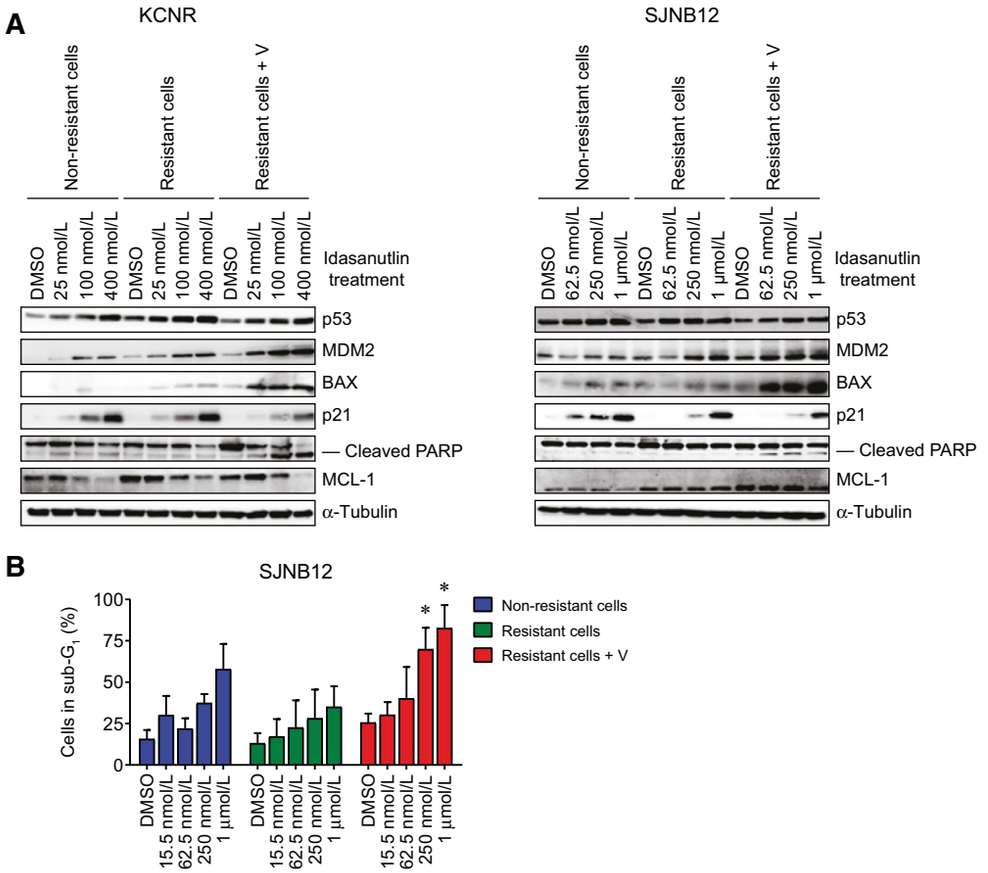

Figure 4.

In vitro idasanutlin treatment of venetoclax-resistant neuroblastoma cells under venetoclax pressure causes BAX-mediated apoptosis. **A,** Western blot analysis of the effects of idasanutlin on p53, MDM2, BAX, p21, cleaved PARP, and MCL-1 protein levels in non-resistant KCNR (left) and SJNB12 (right) cells versus venetoclax-resistant KCNR and SJNB12 cells in the absence and presence of venetoclax after 72 hours treatment. α-Tubulin was used as a loading control. **B,** FACS analysis of the effects of idasanutlin on sub-G_1 induction in non-resistant SJNB12 cells (blue) versus venetoclax-resistant SJNB12 cells (green) and venetoclax-resistant SJNB12 cells in the presence of venetoclax (red). Effects on sub-G_1 induction were established after 72 hours treatment with increasing idasanutlin concentrations. Data represent the mean percentage of cells in sub-G_1 + SD of three replicate experiments. Significance between treatment groups receiving the same concentration of idasanutlin was calculated using a one-way ANOVA. Significant effects (*, $P < 0.05$) were only obtained at 250 nmol/L and 1 µmol/L concentrations of idasanutlin for the resistant cells in the presence of venetoclax compared to the resistant cells without venetoclax. +V = venetoclax IC_{85} concentration (KCNR, 7.5 µmol/L and SJNB12, 2.75 µmol/L).

Venetoclax and idasanutlin combination therapy causes tumor regression in a patient-derived BCL-2–dependent neuroblastoma xenograft model

As PDX models have shown to better recapitulate the biological and molecular characteristics of the original patient tumor (37), the effects of venetoclax–idasanutlin combination treatment were tested against a BCL-2–dependent PDX, CHOA-NBX-4. Single-agent treatment with venetoclax or idasanutlin significantly inhibited the growth of CHOA-NBX-4 tumors after 10 days of treatment, with average changes in tumor volume of +232% and +96%, respectively, versus +597% for vehicle control mice (**Fig. 6A**; Supplementary Fig. S4B). Although the p53 status of CHOA-NBX-4 is still under investigation, its sensitivity toward idasanutlin indicates that this model is p53 wild-type. In line with the classical xenograft model KCNR, combination treatment of CHOA-NBX-4 PDXs was superior to single-agent treatment with an average percentage change in tumor volume of −72% (Supplementary Fig. S4B). 10 days of combination therapy resulted in five PRs (5/6), whereas the best response for both monotherapies was one case of stable disease (1/5 for venetoclax and 1/4 for idasanutlin; Supplementary Fig. S4C). BIM/BCL-2–binding patterns were similar to the patterns observed in classical KCNR xenografts, showing BIM release following addition of venetoclax as a single-agent therapy, as well as, in combination with idasanutlin (**Fig. 6B**). Interestingly, CHOA-NBX-4 tumors treated with venetoclax monotherapy were not affected by MCL-1–mediated resistance, as demonstrated by the lack of BIM/MCL-1 complex levels in any of the treatment arms (**Fig. 6B**). In line with *in vitro* observations, idasanutlin increased p53 and MDM2 levels when given alone and in combination with venetoclax (**Fig. 6C**). Increased p53 levels were accompanied by upregulated levels of BAX, a known activation target of p53. BIM release upon venetoclax binding to BCL-2 and elevated levels of p53 and BAX upon idasanutlin binding to MDM2 explain the strong apoptotic response confirmed upon combination therapy by increased cleaved PARP levels (**Fig. 6B** and **C**).

Effects of venetoclax–idasanutlin combination therapy were additionally studied in a second BCL-2–dependent p53 wild-type PDX model, COG-N-424x. Unfortunately, none of the treatment strategies

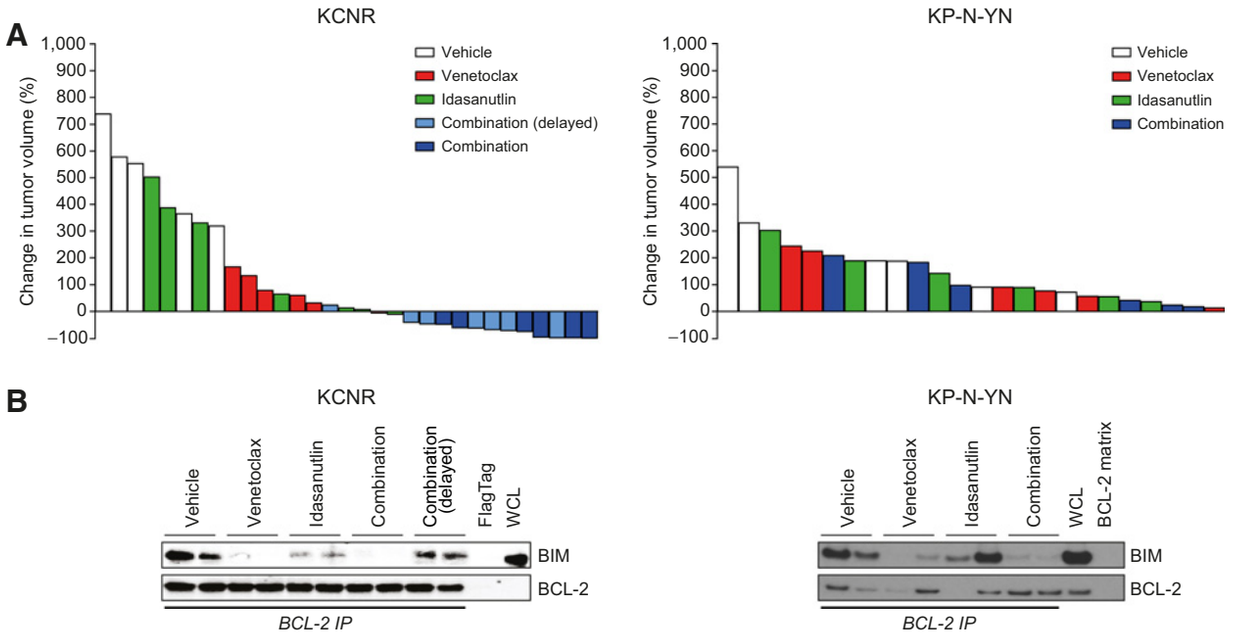

Figure 5.

In vivo effects of venetoclax in combination with idasanutlin in classical neuroblastoma xenograft mouse models. **A,** Waterfall plots of the percentage change in tumor volume in the KCNR (left) and KP-N-YN (right) neuroblastoma xenograft model. Mice were treated with either vehicle, venetoclax monotherapy (100 mg/kg/day), idasanutlin monotherapy (25 mg/kg/day) or venetoclax in combination with idasanutlin for three consecutive weeks. For the KCNR xenograft model, an extra group was included, in which mice first received one-week venetoclax monotherapy followed by two weeks combination treatment (delayed combination). The percentage change in tumor volume was calculated using the following formula: [(tumor volume at the end of treatment—tumor volume at the start of treatment)/tumor volume at the start of treatment] × 100%. **B,** *In vivo* effects on BIM release from BCL-2 for the KCNR (left) and KP-N-YN (right) neuroblastoma xenograft model. BIM/BCL-2 complex levels were detected by anti–BCL-2 immunoprecipitation (IP), followed by western blotting for BIM. BIM/BCL-2 complex levels were established for $n = 2$ mice per group after treatment completion (KCNR) or after 7 days of treatment (KP-N-YN), using tumor material harvested 4 hours after administration of the last dose. WCL, whole-cell lysate.

(venetoclax monotherapy, idasanutlin monotherapy or combination therapy) led to statistically significant differences in the average change in tumor volume (+193%, +185%, and +178%, respectively) compared with the vehicle-treated mice (+216%; **Fig. 6A**; Supplementary Fig. S4B). Because COG-N-424x mice did not complete the 21-day treatment cycle due to tumor burden, group comparison was performed after a suboptimal period of only four days of treatment to have sufficient mice available in each treatment arm. Additional waterfall plots with tumor volumes at the last day of treatment confirm no responses to treatment (Supplementary Fig. S4D). Despite the lack of significant effects on COG-N-424 tumor sizes, some of the observed biochemical effects were surprisingly similar to responding tumors. Combination therapy led to enhanced PARP cleavage, and both p53 and MDM2 were upregulated after idasanutlin monotherapy and combination therapy (**Fig. 6C**). In addition, BIM/BCL-2 co-immunoprecipitation studies demonstrated BIM displacement after venetoclax monotherapy and combination therapy. In line with tumors non-responsive to venetoclax therapy, overall levels of BIM bound to BCL-2 were very low (**Fig. 6B**; Supplementary Fig. S5B). In addition, BIM was not bound to MCL-1 in vehicle-treated and monotherapy-treated mice, but high BIM/MCL-1 complex levels were observed after combination therapy (**Fig. 6B**).

Discussion

Preclinical studies using the BCL-2–specific inhibitor venetoclax demonstrate antitumor activity in neuroblastoma tumors with high BCL-2 and BIM/BCL-2 complex levels (18, 38). However, acquired resistance develops following venetoclax therapy, as is commonly seen with highly specific targeted compounds, which ultimately limits its usefulness as a single-agent treatment strategy (18, 39).

We previously established that acquired venetoclax resistance in neuroblastoma cells coincides with upregulation of MCL-1 and BIM relocation to MCL-1 (18). Similar effects were confirmed for the venetoclax-resistant neuroblastoma cell lines in this study. Upregulation of other anti-apoptotic BCL-2 family members was shown to play a pivotal role in neuroblastoma resistance to venetoclax. This was further supported by the absence of mutations in the BH3 domain of BCL-2. The development of MCL-1–mediated resistance to venetoclax suggests that a combination with MCL-1 inhibitors will enhance therapeutic effectiveness. Indeed, preliminary studies have revealed promising apoptotic effects upon simultaneous inhibition of BCL-2 and MCL-1 in BCL-2-dependent neuroblastoma models (18). However, MCL-1 inhibitors are still in early clinical development, limiting rapid translation of the combined strategy into the clinic. Considering the promise of venetoclax, which is already under clinical investigation (NCT03236857), we aimed to discover alternative combinatorial strategies for fast clinical implementation. To this end, we performed a screen with multiple approved drugs and promising targeted drugs in clinical or late preclinical development to identify compounds that resensitize neuroblastoma cells with acquired resistance to venetoclax.

Interestingly, we found numerous compounds targeting the IGF-1R/PI3K/mTOR axis in the drug screen hits, indicating potential for combining venetoclax with an inhibitor of this drug class. These

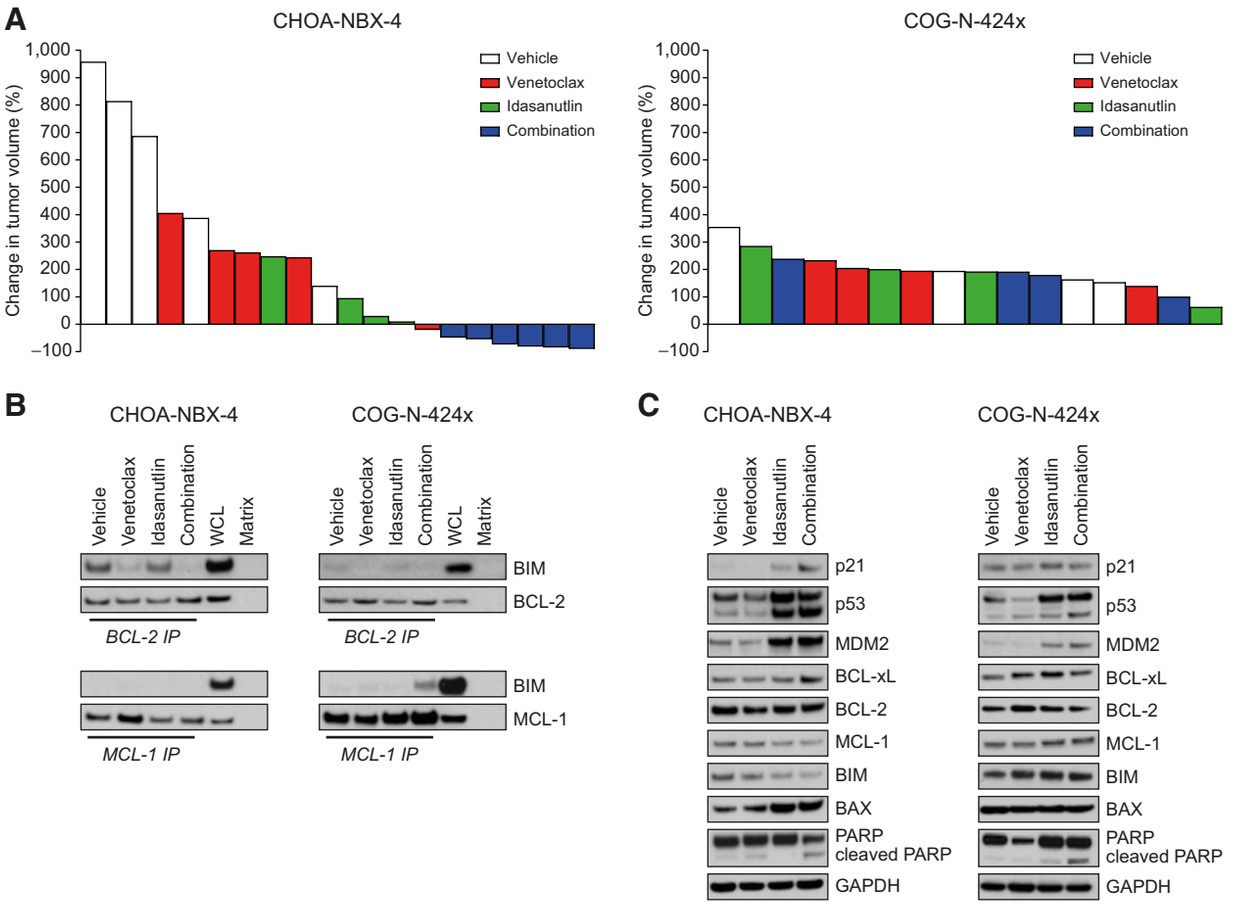

Figure 6.

In vivo effects of venetoclax in combination with idasanutlin in neuroblastoma patient-derived xenograft (PDX) mouse models. **A,** Waterfall plots of the percentage change in tumor volume in the CHOA-NBX-4 (left) and COG-N-424x (right) PDX model. Mice were treated with either vehicle, venetoclax monotherapy (100 mg/kg/day), idasanutlin monotherapy (25 mg/kg/day) or venetoclax in combination with idasanutlin. The percentage change in tumor volume was calculated using the following formula: [(tumor volume at the end of treatment—tumor volume at the start of treatment)/tumor volume at the start of treatment] × 100%. Waterfall plots were established using tumor volumes obtained 10 days after treatment initiation (CHOA-NBX-4) or 4 days after treatment initiation (COG-N-424x). **B,** *In vivo* effects on BIM release from BCL-2 and BIM capturing by MCL-1 for the CHOA-NBX-4 (left, day 3) and COG-N-424x (right, day 7) PDX model. BIM/BCL-2 and BIM/MCL-1 complex levels were established by immunoprecipitation of BCL-2 or MCL-1, respectively, followed by western blotting for BIM. **C,** Western blot analysis of the *in vivo* effects of venetoclax and idasanutlin alone or in combination on p21, p53, MDM2, BCL-X_L, BCL-2, MCL-1, BIM, BAX and cleaved PARP in the CHOA-NBX-4 (left, day 3) and COG-N-424x (right, day 7) PDX model at 4 hours after drug administration. GAPDH was used as a loading control. WCL, whole-cell lysate.

combinations have indeed been described before to result in synergistic or additive effects on cell death in various types of cancers, including chronic lymphocytic leukemia, non-Hodgkin lymphoma, multiple myeloma, and acute myelogenous leukemia (40). However, these favorable combined effects still have to be confirmed in neuroblastoma. Our drug screen furthermore revealed that ALK inhibitors could restore the sensitivity to venetoclax in resistant neuroblastoma cells with an ALK-mutated background. Because ALK mutations are frequently detected in patients with neuroblastoma, our data provide further support for combining venetoclax with an ALK inhibitor (41, 42). Despite these interesting findings, we decided to focus on drugs resensitizing both venetoclax-resistant neuroblastoma model systems, to ensure that a larger patient population might benefit from treatment with the identified drug combination. Targeted compounds idasanutlin, omipalisib, flavopiridol, vorinostat, and the cytostatic doxorubicin demonstrated superior antitumor activity in venetoclax-resistant KCNR and SJNB12 cells compared with their non-resistant ancestor cell lines, thereby confirming previously reported favorable combinations with BCL-2 inhibitors (20, 25–31). Further validation of number one hit idasanutlin confirmed its potential in restoring sensitivity of neuroblastoma cells to venetoclax. On the basis of the differences in idasanutlin dose–response curves and IC_{50} values for resistant neuroblastoma cell lines in the absence versus presence of venetoclax, resensitizing effects of idasanutlin seem to be much more pronounced for SJNB12 compared with KCNR. However, western blot analysis showed that idasanutlin monotherapy led to cell-cycle arrest in venetoclax-resistant cells in the absence of venetoclax, while causing a strong apoptotic response for both venetoclax-resistant KCNR and SJNB12 cells in the presence of venetoclax. These results indicate that resensitization is also occurring in KCNR, despite the limited differences observed in the percentage viable cells. However, our *in vitro* validation studies did show a surprising difference in the mechanism of action for idasanutlin between KCNR and SJNB12 cells. Although causing MCL-1 downregulation in normal KCNR cells and

venetoclax-resistant KCNR cells in the absence and presence of venetoclax, idasanutlin treatment of SJNB12 only resulted in a modest decrease in MCL-1 expression in the non-resistant cells with no effects in both venetoclax-resistant conditions. These inconsistent effects of idasanutlin on MCL-1 protein levels are in line with previously published observations. Although Lehmann and colleagues (24) and Pan and colleagues (43) reported that idasanutlin promotes MCL-1 degradation, no effects of idasanutlin on MCL-1 were observed by Van Goethem and colleagues (44).

Differences in response to idasanutlin treatment might be due to variations in the genetic background of the tested model systems and/or more complex interactions between multiple involved pathways. All model systems used in the current study are p53 wild-type, which is crucial for the anticancer activity of idasanutlin. In addition, KCNR is a MYCN-amplified neuroblastoma cell line harboring an activating mutation in ALK, whereas SJNB12 is MYCN and ALK wild-type. Both MYCN and ALK are well-known oncodriver genes in neuroblastoma.

Superior apoptotic responses upon venetoclax–idasanutlin combination therapy were confirmed *in vivo*. These findings are supported by a study of Van Goethem and colleagues (44) in which venetoclax was identified as a synergistic interaction partner of idasanutlin. Our study revealed that antitumor effects observed after venetoclax–idasanutlin combination therapy were caused by a dual effect on the intrinsic apoptotic pathway: BIM release from BCL-2 caused by venetoclax and p53-mediated BAX activation by idasanutlin. This combination of apoptotic effects led to tumor regression, including one CR (Supplementary Figs. S3B, S3C, S4B, and S4C) and increased survival chances (Supplementary Figs. S3A and S4A) in two neuroblastoma xenograft models. Longer studies investigating repeated cycles of venetoclax–idasanutlin combination therapy are required to estimate whether combination therapy with two targeted compounds is sufficient to achieve sustained tumor regression (Supplementary Figs. S3C and S4C).

Combination therapy with venetoclax and idasanutlin was not effective in two other neuroblastoma xenograft models tested. This may be explained by their lower BCL-2 dependency and the occurrence of MCL-1–mediated resistance. KP–N–YN is a BCL-2–dependent cell line (Supplementary Fig. S6), but the xenograft model generated from these cells showed unexpected variation in baseline levels of BCL-2 and BIM/BCL-2 complex (**Fig. 5B**; Supplementary Fig. S5A). Similarly, only limited BIM/BCL-2 complex levels could be detected in COG-N-424x PDXs, despite the observation that BIM was only bound to BCL-2 and not to the anti-apoptotic proteins MCL-1 or BCL-X_L (**Fig. 6B**; Supplementary Fig. S5B and S5C). Previously, we and others found that high BCL-2- and BIM/BCL-2 complex levels are biomarkers of efficacy for venetoclax therapy (18, 38). Observed variable or low levels of BCL-2 in KP–N–YN and COG-N-424x xenografts might therefore be one explanation for their lack of response to venetoclax–idasanutlin combination therapy. Baseline BIM/MCL-1 complex levels in KP–N–YN xenografts and massive increases in BIM/MCL-1 complex levels observed in both non-responsive xenograft models upon combination therapy with venetoclax and idasanutlin might be another explanation (**Fig. 6B**; Supplementary Fig. S3E). Finally, as shortly addressed above, the *in vitro* observations that idasanutlin led to variable effects on MCL-1 and induced apoptosis in venetoclax-resistant cells kept under venetoclax pressure while only causing cell-cycle arrest when venetoclax was removed, suggest the involvement of more complex interactions that might explain the differences in therapy response.

In conclusion, our results indicate that idasanutlin is a potential drug candidate for resensitizing venetoclax-resistant neuroblastoma cells to venetoclax. This preclinical data provide further rationale for the ongoing clinical trial testing the combination of venetoclax and idasanutlin in pediatric cancers, including neuroblastoma (NCT04029688). On the basis of our data, we predict that a subset of BCL-2–dependent patients with neuroblastoma will benefit from a combination of venetoclax and idasanutlin. However, the current study also underlines the importance of finding relevant biomarkers of efficacy for this combination to prevent unnecessary clinical failures and offer potential non-responders better alternatives.

Authors' Disclosures

D. Lelieveld reports other from Genmab outside the submitted work. D.A. Egan reports other from Core Life Analytics outside the submitted work. M. Kerstjens reports grants from Stichting KiKa during the conduct of the study, personal fees from Janssen Vaccines Leiden outside the submitted work. No disclosures were reported by the other authors.

Authors' Contributions

L. Vernooij: Formal analysis, validation, investigation, visualization, methodology, writing–original draft, project administration, writing–review and editing. **L.T. Bate-Eya:** Formal analysis, validation, investigation, visualization, methodology, writing–original draft, writing–review and editing. **L.K. Alles:** Formal analysis, validation, investigation, methodology. **J.Y. Lee:** Formal analysis, validation, investigation, visualization, writing–original draft. **B. Koopmans:** Validation, investigation, methodology. **H.C. Jonus:** Validation, investigation, visualization, writing–review and editing. **N.A. Schubert:** Validation, investigation, visualization. **L. Schild:** Validation, investigation. **D. Lelieveld:** Resources, methodology. **D.A. Egan:** Resources, methodology. **M. Kerstjens:** Resources. **R.W. Stam:** Resources. **J. Koster:** Data curation, software. **K.C. Goldsmith:** Conceptualization, resources, methodology, writing–review and editing. **J.J. Molenaar:** Conceptualization, supervision, funding acquisition, methodology, writing–review and editing. **M.E.M. Dolman:** Conceptualization, formal analysis, supervision, funding acquisition, validation, visualization, methodology, writing–original draft, project administration, writing–review and editing.

Acknowledgements

The research in this article was supported by grants from the Villa Joep Foundation (grant BCL-2 in neuroblastoma), the Kinderen Kankervrij Foundation (KiKa; grant 189), ERC-START (grant PREDICT-716079), NWO-Vidi (grant 91716482) and Aflac Pilot grant (to K.C. Goldsmith). We would like to thank Dr. C. Patrick Reynolds and Cogcell.org for providing us with the COG-N-424x PDX model and the CHOA Pediatric Biorepository for the CHOA-NBX-4 PDX model.

The costs of publication of this article were defrayed in part by the payment of page charges. This article must therefore be hereby marked *advertisement* in accordance with 18 U.S.C. Section 1734 solely to indicate this fact.

Received August 5, 2020; revised December 9, 2020; accepted March 23, 2021; published first April 13, 2021.

References

1. Yip KW, Reed JC. Bcl-2 family proteins and cancer. Oncogene 2008;27:6398–406.
2. Czabotar PE, Lessene G, Strasser A, Adams JM. Control of apoptosis by the BCL-2 protein family: implications for physiology and therapy. Nat Rev Mol Cell Biol 2014;15:49–63.
3. Iqbal J, Neppalli VT, Wright G, Dave BJ, Horsman DE, Rosenwald A, et al. BCL2 expression is a prognostic marker for the activated B-cell-like type of diffuse large B-cell lymphoma. J Clin Oncol 2006;24:961–8.
4. Davids MS, Letai A. Targeting the B-cell lymphoma/leukemia 2 family in cancer. J Clin Oncol 2012;30:3127–35.

5. Hu W, Kavanagh JJ. Anticancer therapy targeting the apoptotic pathway. Lancet Oncol 2003;4:721–9.
6. Korsmeyer SJ, Wei MC, Saito M, Weiler S, Oh KJ, Schlesinger PH. Pro-apoptotic cascade activates BID, which oligomerizes BAK or BAX into pores that result in the release of cytochrome c. Cell Death Differ 2000;7:1166–73.
7. Saelens X, Festjens N, Vande Walle L, van Gurp M, van Loo G, Vandenabeele P. Toxic proteins released from mitochondria in cell death. Oncogene 2004;23: 2861–74.
8. Sun XM, MacFarlane M, Zhuang J, Wolf BB, Green DR, Cohen GM. Distinct caspase cascades are initiated in receptor-mediated and chemical-induced apoptosis. J Biol Chem 1999;274:5053–60.
9. Tait SW, Green DR. Mitochondria and cell death: outer membrane permeabilization and beyond. Nat Rev Mol Cell Biol 2010;11:621–32.
10. Wei MC, Lindsten T, Mootha VK, Weiler S, Gross A, Ashiya M, et al. tBID, a membrane-targeted death ligand, oligomerizes BAK to release cytochrome c. Genes Dev 2000;14:2060–71.
11. Chipuk JE, Moldoveanu T, Llambi F, Parsons MJ, Green DR. The BCL-2 family reunion. Mol Cell 2010;37:299–310.
12. Green DR, Kroemer G. The pathophysiology of mitochondrial cell death. Science 2004;305:626–9.
13. Llambi F, Moldoveanu T, Tait SW, Bouchier-Hayes L, Temirov J, McCormick LL, et al. A unified model of mammalian BCL-2 protein family interactions at the mitochondria. Mol Cell 2011;44:517–31.
14. Goldsmith KC, Gross M, Peirce S, Luyindula D, Liu X, Vu A, et al. Mitochondrial Bcl-2 family dynamics define therapy response and resistance in neuroblastoma. Cancer Res 2012;72:2565–77.
15. Lamers F, Schild L, den Hartog IJ, Ebus ME, Westerhout EM, Ora I, et al. Targeted BCL2 inhibition effectively inhibits neuroblastoma tumour growth. Eur J Cancer 2012;48:3093–103.
16. Irwin MS, Park JR. Neuroblastoma: paradigm for precision medicine. Pediatr Clin North Am 2015;62:225–56.
17. Souers AJ, Leverson JD, Boghaert ER, Ackler SL, Catron ND, Chen J, et al. ABT-199, a potent and selective BCL-2 inhibitor, achieves antitumor activity while sparing platelets. Nat Med 2013;19:202–8.
18. Bate-Eya LT, den Hartog IJ, van der Ploeg I, Schild L, Koster J, Santo EE, et al. High efficacy of the BCL-2 inhibitor ABT199 (venetoclax) in BCL-2 high-expressing neuroblastoma cell lines and xenografts and rational for combination with MCL-1 inhibition. Oncotarget 2016;7:27946–58.
19. McCurrach ME, Connor TM, Knudson CM, Korsmeyer SJ, Lowe SW. bax-deficiency promotes drug resistance and oncogenic transformation by attenuating p53-dependent apoptosis. Proc Natl Acad Sci U S A 1997;94:2345–9.
20. Choudhary GS, Al-Harbi S, Mazumder S, Hill BT, Smith MR, Bodo J, et al. MCL-1 and BCL-xL-dependent resistance to the BCL-2 inhibitor ABT-199 can be overcome by preventing PI3K/AKT/mTOR activation in lymphoid malignancies. Cell Death Dis 2015;6:e1593.
21. Fresquet V, Rieger M, Carolis C, Garcia-Barchino MJ, Martinez-Climent JA. Acquired mutations in BCL2 family proteins conferring resistance to the BH3 mimetic ABT-199 in lymphoma. Blood 2014;123:4111–9.
22. Dolman ME, Poon E, Ebus ME, den Hartog IJ, van Noesel CJ, Jamin Y, et al. Cyclin-dependent kinase inhibitor AT7519 as a potential drug for MYCN-dependent neuroblastoma. Clin Cancer Res 2015;21:5100–9.
23. Ding Q, Zhang Z, Liu JJ, Jiang N, Zhang J, Ross TM, et al. Discovery of RG7388, a potent and selective p53-MDM2 inhibitor in clinical development. J Med Chem 2013;56:5979–83.
24. Lehmann C, Friess T, Birzele F, Kiialainen A, Dangl M. Superior anti-tumor activity of the MDM2 antagonist idasanutlin and the Bcl-2 inhibitor venetoclax in p53 wild-type acute myeloid leukemia models. J Hematol Oncol 2016;9:50.
25. Cervantes-Gomez F, Lamothe B, Woyach JA, Wierda WG, Keating MJ, Balakrishnan K, et al. Pharmacological and protein profiling suggests venetoclax (ABT-199) as optimal partner with ibrutinib in chronic lymphocytic leukemia. Clin Cancer Res 2015;21:3705–15.
26. Li L, Pongtornpipat P, Tiutan T, Kendrick SL, Park S, Persky DO, et al. Synergistic induction of apoptosis in high-risk DLBCL by BCL2 inhibition with ABT-199 combined with pharmacologic loss of MCL1. Leukemia 2015;29: 1702–12.
27. Johnson-Farley N, Veliz J, Bhagavathi S, Bertino JR. ABT-199, a BH3 mimetic that specifically targets Bcl-2, enhances the antitumor activity of chemotherapy, bortezomib and JQ1 in "double hit" lymphoma cells. Leuk Lymphoma 2015;56: 2146–52.
28. Vandenberg CJ, Cory S. ABT-199, a new Bcl-2-specific BH3 mimetic, has in vivo efficacy against aggressive Myc-driven mouse lymphomas without provoking thrombocytopenia. Blood 2013;121:2285–8.
29. Benito JM, Godfrey L, Kojima K, Hogdal L, Wunderlich M, Geng H, et al. MLL-rearranged acute lymphoblastic leukemias activate BCL-2 through H3K79 methylation and are sensitive to the BCL-2-specific antagonist ABT-199. Cell Rep 2015;13:2715–27.
30. Wei Y, Kadia T, Tong W, Zhang M, Jia Y, Yang H, et al. The combination of a histone deacetylase inhibitor with the Bcl-2 homology domain-3 mimetic GX15–070 has synergistic antileukemia activity by activating both apoptosis and autophagy. Clin Cancer Res 2010;16:3923–32.
31. Xie S, Jiang H, Zhai XW, Wei F, Wang SD, Ding J, et al. Antitumor action of CDK inhibitor LS-007 as a single agent and in combination with ABT-199 against human acute leukemia cells. Acta Pharmacol Sin 2016;37:1481–9.
32. Chen L, Rousseau RF, Middleton SA, Nichols GL, Newell DR, Lunec J, et al. Pre-clinical evaluation of the MDM2-p53 antagonist RG7388 alone and in combination with chemotherapy in neuroblastoma. Oncotarget 2015;6:10207–21.
33. Lakoma A, Barbieri E, Agarwal S, Jackson J, Chen Z, Kim Y, et al. The MDM2 small-molecule inhibitor RG7388 leads to potent tumor inhibition in p53 wild-type neuroblastoma. Cell Death Discov 2015;1:15026.
34. Nag S, Qin J, Srivenugopal KS, Wang M, Zhang R. The MDM2-p53 pathway revisited. J Biomed Res 2013;27:254–71.
35. Kracikova M, Akiri G, George A, Sachidanandam R, Aaronson SA. A threshold mechanism mediates p53 cell fate decision between growth arrest and apoptosis. Cell Death Differ 2013;20:576–88.
36. Chipuk JE, Kuwana T, Bouchier-Hayes L, Droin NM, Newmeyer DD, Schuler M, et al. Direct activation of Bax by p53 mediates mitochondrial membrane permeabilization and apoptosis. Science 2004;303:1010–4.
37. Koga Y, Ochiai A. Systematic review of patient-derived xenograft models for preclinical studies of anti-cancer drugs in solid tumors. Cells 2019;8:418.
38. Tanos R, Karmali D, Nalluri S, Goldsmith KC. Select Bcl-2 antagonism restores chemotherapy sensitivity in high-risk neuroblastoma. BMC Cancer 2016;16:97.
39. Groenendijk FH, Bernards R. Drug resistance to targeted therapies: deja vu all over again. Mol Oncol 2014;8:1067–83.
40. Leverson JD, Sampath D, Souers AJ, Rosenberg SH, Fairbrother WJ, Amiot M, et al. Found in translation: how preclinical research is guiding the clinical development of the BCL2-selective inhibitor venetoclax. Cancer Discov 2017; 7:1376–93.
41. Chen Y, Takita J, Choi YL, Kato M, Ohira M, Sanada M, et al. Oncogenic mutations of ALK kinase in neuroblastoma. Nature 2008;455:971–4.
42. Trigg RM, Turner SD. ALK in neuroblastoma: biological and therapeutic implications. Cancers 2018;10:113.
43. Pan R, Ruvolo V, Mu H, Leverson JD, Nichols G, Reed JC, et al. Synthetic lethality of combined Bcl-2 inhibition and p53 activation in AML: mechanisms and superior antileukemic efficacy. Cancer Cell 2017;32:748–60.
44. Van Goethem A, Yigit N, Moreno-Smith M, Vasudevan SA, Barbieri E, Speleman F, et al. Dual targeting of MDM2 and BCL2 as a therapeutic strategy in neuroblastoma. Oncotarget 2017;8:57047–57.